Effect of Γ-*X* interband mixing on the surface electronic structure of GaAs/AlAs superlattices

B. Brzostowski and R. Kucharczyk*
Institute of Experimental Physics, University of Wrocław, plac Maksa Borna 9, 50–204 Wrocław, Poland
(Received 21 October 2002; revised manuscript received 6 January 2003; published 14 March 2003)

The envelope-function description of short-period $Al_xGa_{1-x}As$-based superlattices (SL's), taking into account the elastic Γ-*X* intervalley transfer by introducing an additional δ-functional scattering potential at each well/barrier heterointerface, is extended to study the surface electronic structure of a terminated GaAs/AlAs SL. Modification of the energy spectrum and the localization properties of SL surface states with respect to previous single-band treatments is clearly indicated, and identified as a result of the Γ-*X* interband coupling.

DOI: 10.1103/PhysRevB.67.125305 PACS number(s): 73.21.−b, 73.20.At

I. INTRODUCTION

It is well established that the lowest conduction minibands of GaAs/AlAs superlattices (SL's) with sufficiently long period and/or thin AlAs barrier layers are entirely determined by Γ-valley states of GaAs. Therefore, the common one-band envelope-function approximation with rectangular (Kronig–Penney-like) potential profile, corresponding to the Γ-Γ intervalley offset, is suitable to describe the bulk electronic structure of such SL's in the conduction-band-bottom energy range.[1,2] Accordingly, the *surface* electronic structure of *terminated* long-period SL's—in particular, the experimentally observed spectrum of SL surface states[3,4]—can be appropriately reproduced by the respective semi-infinite one-band Kronig–Penney-type of model (see Ref. 5, and references therein).

For short-period SL's, however, the minibands originating from *X*-valley states of AlAs become lowest in energy, and hence, must be additionally taken into account within any reliable treatment of such systems.[6] Moreover, in many instances, the Γ-*X* interband mixing plays a crucial role for a correct interpretation of the observed electronic, optical, and transport characteristics of $Al_xGa_{1-x}As$-based heterostructures.[7–13] Nevertheless, the relevance of this effect has never been addressed with respect to the *surface* electronic properties of SL's. Consequently, in this paper we examine the influence of the coupling between the Γ-derived and *X*-derived minibands on the energy spectrum and localization properties of surface states of an $Al_yGa_{1-y}As$-terminated GaAs/AlAs SL, indicating a possibility of their important modification as compared to the results of earlier single-band approaches.

II. MODEL AND METHOD

The energy positions of the conduction-band minima of bulk $Al_xGa_{1-x}As$ at the Γ and *X* points, relative to the conduction-band bottom of GaAs, depend on the Al mole fraction *x* according to[14]

$$V_\Gamma(x) = (911x + 147x^2)\ \text{meV} \tag{1a}$$

and

$$V_X(x) = (473 - 295x)\ \text{meV}, \tag{1b}$$

while the effective masses of electrons in the respective valleys are given by[14]

$$m_\Gamma^*(x) = (0.067 + 0.083x)m_0 \tag{2a}$$

and

$$m_X^*(x) = (1.3 - 0.2x)m_0, \tag{2b}$$

m_0 being the free electron mass.[15] In the SL sequence, the Γ-Γ and *X*-*X* intervalley offsets between GaAs and AlAs result in Kronig–Penney-like potential profiles $V_\Gamma(z)$ and $V_X(z)$ along the SL axis *z*, correspondingly, as sketched in Fig. 1. This means that the GaAs and AlAs (AlAs and GaAs) layers constitute quantum wells (barriers) for Γ-valley and *X*-valley electrons, respectively.

The considered SL is terminated by an $Al_yGa_{1-y}As$ clad layer, leading to the formation of the so-called *internal surface* at the SL/clad-layer interface,[3–5] to which we hereafter refer simply as the SL surface (cf. Fig. 1). According to Eqs. (1), varying the Al mole fraction *y* in the clad layer influences simultaneously the heights V_Γ^S and V_X^S of the terminating potential steps for the Γ-Γ and *X*-*X* profiles, thus offering a means of modifying the SL surface conditions.

The structure depicted in Fig. 1 is described by a two-band effective-mass model.[16–18] In this approximation, the electronic wave function has two components, ψ_Γ and ψ_X, representing the envelope functions associated with the Γ and *X* valleys. Since no elastic transfer between the Γ-valley and *X*-valley states is allowed in the bulk of semiconductors composing the SL, these envelopes are independent of each other within any of the SL layers, and consequently, satisfy conventional Schrödinger equations with appropriate potential profiles and effective masses,[7,16] viz.,

$$-\frac{\hbar^2}{2}\frac{\partial}{\partial z}\left[\frac{1}{m_{\Gamma,X}^*(z)}\frac{\partial\psi_{\Gamma,X}(z)}{\partial z}\right] + V_{\Gamma,X}(z)\,\psi_{\Gamma,X}(z) = E\,\psi_{\Gamma,X}(z). \tag{3}$$

However, rapid changes of the SL potential at GaAs/AlAs heterojunctions induce elastic scattering between the Γ-valley- and *X*-valley-derived states,[19] and hence, cause a mixing of the envelope-function components ψ_Γ and ψ_X, originally corresponding to distinct energy minibands.[7,16–18,20–22] Since the Γ-*X* intervalley transfer is

 ©2003 The American Physical Society

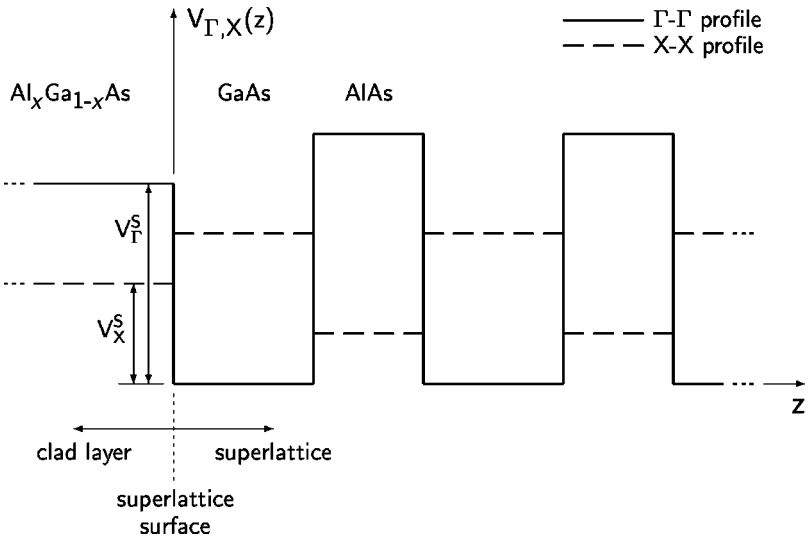

FIG. 1. Potential profiles $V_\Gamma(z)$ (solid line) and $V_X(z)$ (dashed line) for the Γ-valley and X-valley electrons, respectively, of the considered $Al_xGa_{1-x}As$-terminated GaAs/AlAs SL. The Al mole fraction y in the clad layer determines the heights V_Γ^S and V_X^S of the surface potential steps for the Γ-Γ and X-X profiles (see text for details).

strictly confined to the interfaces, in phenomenological approaches it is often taken into account by introducing an additional scattering potential, of the form of Dirac δ function, at each well/barrier heterointerface.[7,13,17,18,20] The use of δ-functional interband coupling has been given a direct justification by an analysis of the corresponding pseudopotential Hamiltonian.[22] Furthermore, such a simple model has proven capable of reproducing experimentally measured mixing effects in $Al_xGa_{1-x}As$-based resonant-tunneling heterostructures[7,13] and all but the shortest-period SL's.[8,9,12]

The interface δ-functional scattering potential merely alters the boundary conditions to be obeyed by the envelope-function components.[7,16–18,20–22] More specifically, while ψ_Γ and ψ_X remain continuous across each heterointerface, the (discontinuous) derivative of ψ_Γ becomes coupled to the value of ψ_X and vice versa,[7,17,18] viz.,

$$[\psi_{\Gamma,X}(z)]_{z_i-}^{z_i+}=0, \tag{4a}$$

$$\left[\frac{1}{m^*_{\Gamma,X}(z)}\frac{\partial\psi_{\Gamma,X}(z)}{\partial z}\right]_{z_i-}^{z_i+}=\frac{2p}{\hbar^2}\psi_{X,\Gamma}(z_i), \tag{4b}$$

where z_i stands for the position of an arbitrary SL interface, while p, being the δ-function strength, represents the amount of Γ-X mixing. For the considered semi-infinite SL, the above requirements also apply to envelope-function matching at the SL surface (cf. Fig. 1).

The energy spectrum of surface states for a SL with coupled Γ and X minibands can be derived by a straightforward extension of the direct wave-function matching procedure known from one-band models of terminated SL's.[5] Imposing the boundary conditions (4) and the standard Bloch requirement on the solutions ψ_Γ and ψ_X of the Schrödinger equation (3) over one SL period yields the bulk dispersion relation of a SL, as well as both envelope-function components of the respective eigenstates.[23] For the purpose of the surface-electronic-structure study, however, we do not restrict ourselves to *real* Bloch wave vectors k, appropriate for *extended* states forming energy minibands of an *infinite* SL, but consider the whole *complex band structure*,[24,25] in particular, the analytical continuations of the dispersion curves $E(k)$ for k *complex*, corresponding to wave functions decaying into the SL bulk, and hence, appropriate for *localized* surface states of a *semi-infinite* SL. Matching the components of such determined (decaying) SL wave functions with complex k to the exponentially evanescent solutions of the Schrödinger equation (3) for Γ and X valleys in the clad barrier, via Eqs. (4) at the SL surface, leads to the surface-state-energy expression, parametrized by the δ-functional interband coupling strength p.

To identify the Γ-like or X-like nature of particular SL states, it is useful to consider the relative contributions of the Γ-valley and X-valley envelope-function components to their total wave functions. For this purpose, the factors θ_Γ and θ_X, defined as

$$\theta_{\Gamma,X}=\frac{\int|\psi_{\Gamma,X}(z)|^2\,dz}{\int(|\psi_\Gamma(z)|^2+|\psi_X(z)|^2)dz}, \tag{5}$$

are introduced as a quantitative measure of the Γ or X character, respectively, of each state.[18] More precisely, the dominant contribution of ψ_Γ (ψ_X), resulting in $\theta_\Gamma\approx1$ and $\theta_X\approx0$ ($\theta_\Gamma\approx0$ and $\theta_X\approx1$), indicates that the considered state is localized selectively within GaAs (AlAs) layers of the SL, so it is entirely determined by just the Γ (X) valley. On the contrary, a comparable contribution of ψ_Γ and ψ_X, resulting in $\theta_\Gamma\approx\theta_X$, indicates a considerable Γ-X hybridization, i.e., an efficient intervalley mixing.

III. RESULTS AND DISCUSSION

The Γ-X hybridization is obviously the strongest whenever the Γ-valley- and X-valley-derived SL states become close in energy. Therefore, this effect has usually been studied for cases corresponding to the Γ-X crossover of the lowest conduction minibands of GaAs/AlAs SL's (cf., e.g., Refs. 17 and 18), but always restricted to *bulk* SL states with real

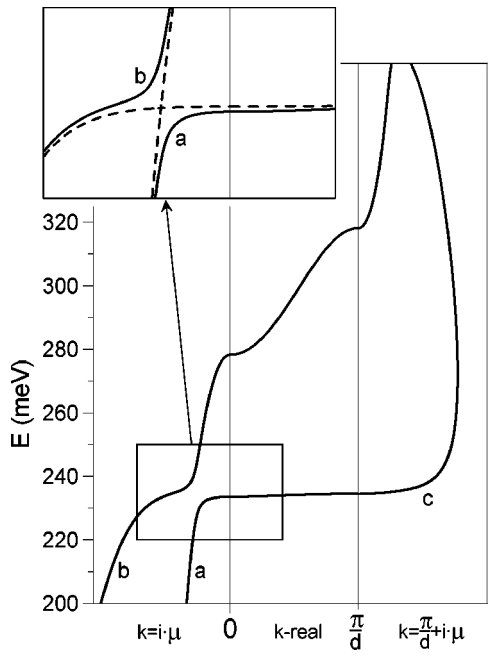

FIG. 2. Complex band structure of the $(GaAs)_8(AlAs)_6$ SL, calculated within a two-band envelope-function model for the δ-functional intervalley scattering potential of strength $p = 0.15$ eVÅ. The range of real $k \in [0, \pi/d]$ (d being the SL period) corresponds to bulk minibands, while the dispersion curves for complex $k = i\mu$ and $k = \pi/d + i\mu$ (μ being real and positive), labeled *a*, *b*, and *c*, are appropriate for localized surface states. Comparison with the results of two independent (i.e., neglecting any interband coupling) one-band models for Γ-Γ (almost vertical dashed line) and *X*-*X* (partially horizontal dashed line) potential profiles is provided in the inset, for the range of energies and wave vectors corresponding to the resonant anticrossing of complex-*k* branches *a* and *b*.

wave vectors *k*. In contrast, in this paper we focus on the interband coupling effect on SL *surface* states with complex *k*, and hence, the system parameters have been chosen such that there is a resonant anticrossing of the *analytical continuations*, i.e., complex-*k* branches, of the Γ-valley- and *X*-valley-related dispersion curves. Consequently, all the calculations have been performed here for a terminated $(GaAs)_8(AlAs)_6$ SL, which exhibits the desired feature.

First, the parameter p of the δ-functional intervalley scattering potential has been determined for the considered SL by comparing the obtained dispersion curves $E(k)$ with those computed within a modern pseudopotential approach.[26,27] The best-fitting procedure yields $p = 0.15$ eVÅ, which agrees with the effective Γ-*X* mixing strength reported elsewhere.[7–10,14,18]

The complex band structure of the $(GaAs)_8(AlAs)_6$ SL, resulting for such a value of p, is shown in Fig. 2. Analysis of the wave functions, according to Eq. (5), of the SL states with real k (which are the only ones allowed in an infinite SL) indicates their prevailing localization within AlAs (GaAs) layers and a clearly X (Γ) character, with $\theta_X > 0.98$ ($\theta_\Gamma > 0.98$), for the first (second) miniband. It means that the first and second minibands originate merely from either the AlAs *X*-valley or the GaAs Γ-valley states, respectively, and thus, the Γ-*X* interband hybridization is negligible in the *bulk* of the considered SL. This is consistent with an almost dispersionless character of the lowest miniband,[28] reflecting a heavy longitudinal mass of *X*-valley electrons [cf. Eq. (2b)], as well as with a relatively large energy gap separating the first and second minibands.

However, a remarkable interaction of the Γ-valley- and *X*-valley-related dispersion curves can be noticed for complex $k = i\mu$ in the energy range around the lowest miniband (cf. branches *a* and *b* in Fig. 2). This clearly avoided-crossing behavior is emphasized in the inset to Fig. 2 by contrasting with the results of two fully independent, i.e., neglecting any interband coupling, one-band models for Γ-Γ and *X*-*X* potential profiles. Consequently, a considerable influence of the Γ-*X* intervalley mixing on the properties of surface states lying within this range of energies can be expected.

To explore this effect, the surface electronic structure of an $Al_yGa_{1-y}As$-terminated $(GaAs)_8(AlAs)_6$ SL has been computed as a function of the Al mole fraction y in the clad layer, leading to the variation of the surface potential barriers V_Γ^S and V_X^S for the Γ-Γ and *X*-*X* profiles (cf. Fig. 1). The results, presented in Fig. 3, indicate the appearance of true surface-localized levels (labeled *a* and *b*) in the interesting energy range around the lowest miniband.

The important modification of the SL surface electronic structure with respect to the results of standard single-band approaches concerns the number of surface states. To be more specific, Kronig–Penney-like calculations performed for the Γ-Γ profile alone yield a surface state (indicated by a dashed line in Fig. 3), emerging beneath the Γ-valley-derived miniband because of the terminating potential barrier being lower than the SL ones for this profile (cf. solid line in Fig. 1).[5] Similar calculations for the *X*-*X* profile alone give no surface states, which in turn is typical for Kronig–Penney-like potentials truncated at the barrier-type of layer (cf. dashed line in Fig. 1).[5] Since the two independent single-band models for Γ-Γ and *X*-*X* potential profiles provide altogether just one SL surface state for any choice of the clad layer, increasing their number up to two in the present two-band treatment (for a considerable range of surface conditions) can be identified as a pure effect of the Γ-*X* interband coupling.

As can be seen in Fig. 3, the lower surface-state-energy curve, labeled *a*, coincides with that resulting from one-band approximation for small enough values of the Al mole fraction y in $Al_yGa_{1-y}As$ clad layer (namely, for $y \lesssim 0.35$), suggesting that surface state *a* with an energy sufficiently below the first miniband is of a Γ-like nature. The same holds for the surface-state-energy curve *b* at energies sufficiently above the first miniband, i.e., for high enough values of y (namely, for $y \gtrsim 0.45$). The character of both surface states is demonstrated in Fig. 4, where the factors θ_Γ and θ_X, defined by Eq. (5), are plotted against y. It follows from Fig. 4 that indeed, as expected, $\theta_\Gamma^a > 0.98$ for $y < 0.3$ and $\theta_\Gamma^a > 0.9$ up to $y = 0.35$, while, on the other hand, $\theta_\Gamma^b > 0.9$ for $y > 0.45$ and $\theta_\Gamma^b > 0.97$ for $y > 0.5$.

For increasing y, however, surface state *a* approaches and

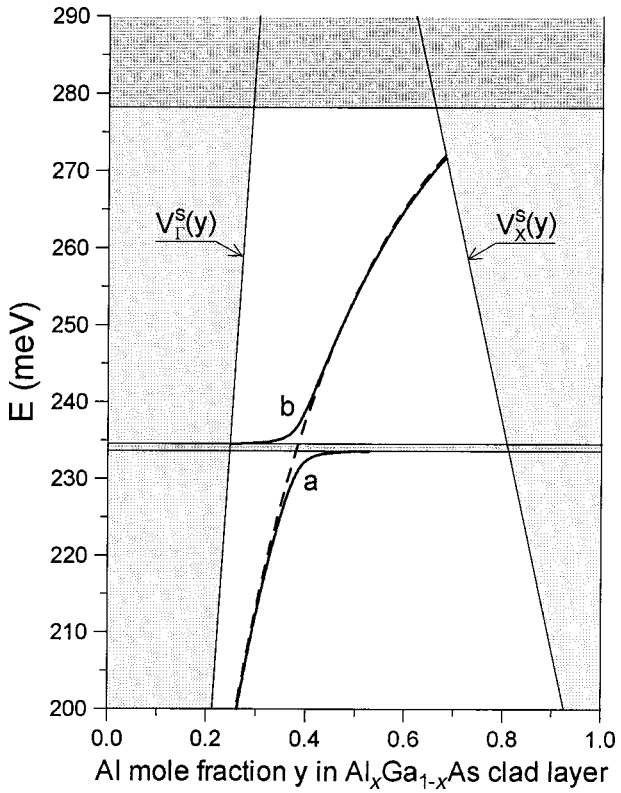

FIG. 3. Surface electronic structure of the $(GaAs)_8(AlAs)_6$ SL terminated by an $Al_yGa_{1-y}As$ clad layer with variable Al mole fraction y. Dark-shaded areas correspond to SL minibands, while thick solid lines (labeled a and b) denote the energy position of surface states, calculated within a two-band model for the δ-functional intervalley scattering potential of strength $p = 0.15$ eVÅ. For comparison, the surface-state-energy position, resulting from the corresponding one-band models neglecting any Γ-X mixing (i.e., for $p=0$), is indicated by a thick dashed line. Thin solid lines depict variation of the terminating barrier heights $V_\Gamma^S(y)$ and $V_X^S(y)$ for the Γ-Γ and X-X potential profile, respectively (cf. Fig. 1), which delimit the energy range for true SL surface states to occur.

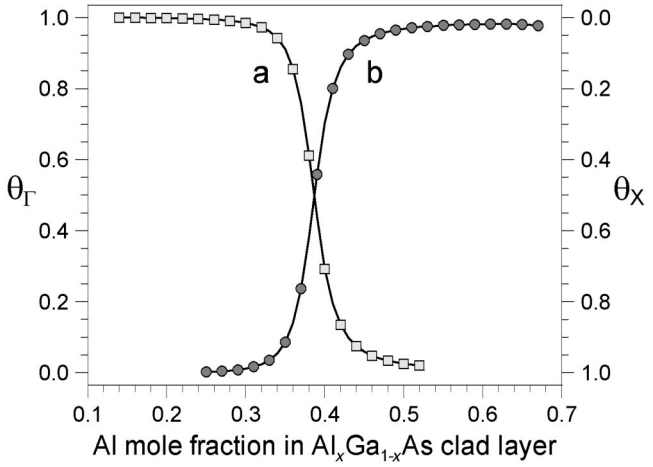

FIG. 4. Factors θ_Γ and θ_X, defined by Eq. (5), plotted as a function of y for surface states a (light-shaded squares) and b (dark-shaded circles) of the $Al_xGa_{1-x}As$-terminated $(GaAs)_8(AlAs)_6$ SL (cf. Fig. 3).

eventually merges into the first (X-like in nature) miniband (cf. Fig. 3), changing consequently its character into predominantly X-like, with $\theta_\Gamma^a < 0.05$, i.e., $\theta_X^a > 0.95$, for $y > 0.45$ (cf. Fig. 4), in accordance with the character of extended states forming the lowest miniband. For smaller values of y, in turn, surface state b is the one lying in the proximity of the miniband edge (cf. Fig. 3), thus exhibiting a clearly X-like nature, with $\theta_X^b > 0.9$ for $y < 0.35$ and $\theta_X^b > 0.98$ for $y < 0.3$ (cf. Fig. 4).

It is noteworthy that the exchange of the character of SL surface states a and b takes place over a relatively narrow range of clad-layer parameters at $y \approx 0.4$. Therefore, their localization properties can be dramatically changed from a dominant confinement in the subsurface GaAs layer to a dominant confinement in the outermost AlAs layer, or vice versa, by just a slight modification of SL surface conditions. For $y \approx 0.4$, both surface-state wave functions exhibit a considerable contribution of Γ-valley, as well as X-valley components, indicating a substantial Γ-X hybridization of surface states. Such a behavior is consistent with the dependences of the dispersion-curve branches a and b, displayed in Fig. 2, and reflects, in particular, their resonant anticrossing at energies around the lowest miniband (cf. inset to Fig. 2).

It is also relevant to examine the extension of particular surface states into the SL bulk. Within one-band approaches, the damping of surface-state wave function is simply given by the imaginary part of the corresponding wave vector.[5] In the two-band model, however, the wave function of a surface state is built of the evanescent solutions from both available complex-k dispersion-curve branches (in our case, branches a and b for surface state a, while branches b and c for surface state b; cf. Figs. 2 and 3), so it is, in general, a linear combination of slower and faster decaying constituents. The relative contribution of these two constituents to the total wave function critically influences the overall spatial distribution of a surface state and, in particular, determines its effective damping towards the SL bulk.

As a consequence, some localization properties of surface states within the present two-band treatment contrast with those known from single-band descriptions of terminated SL's. In the latter case, the degree of surface-state confinement to the SL surface depends solely on its energy position in the minigap, so surface states well separated from the miniband edges are strongly localized at the outermost SL period, while those lying in the vicinity of the miniband always extend deep into the SL bulk, exhibiting a Bloch-like character.[5]

Such a behavior is found here for surface state a, which becomes delocalized when approaching the miniband bottom for $y \approx 0.5$. This is due to the fact that the wave function of surface state a is dominated by the constituent from the dispersion-curve branch a (contribution of the constituent from branch b is negligible for this state), whose imaginary wave vector vanishes at the first miniband bottom (cf. Fig. 2), thus leading to a very slow wave-function decay in the SL direction.

However, surface state b exhibits completely different lo-

calization properties in the proximity of the miniband. For this state, the wave-function constituent from the dispersion-curve branch *b* dominates over that from branch *c*. Since the imaginary part of the respective wave vector is finite for energies around the first miniband top (cf. Fig. 2), surface state *b* remains considerably damped towards the SL bulk at the very edge of the miniband. In fact, it forms there a kind of surface resonance, localized predominantly within one or two outermost AlAs layers (keep in mind that surface state *b* is of clearly *X*-like nature near the top of the first miniband; cf. Fig. 4). Let us emphasize that such a behavior is never observed within standard single-band treatments of terminated SL's.

IV. CONCLUSIONS

As has been shown, the Γ-*X* intervalley mixing affects significantly the surface electronic structure within the conduction-band energy range. In particular, the interband coupling leads to an increased number of SL surface states as compared to the results of earlier models of noninteracting bands. This is in accordance with recent photoemission studies from very-short-period GaAs/AlAs SL's,[29,30] indicating the existence of numerous surface-localized levels for such systems.

Important modifications concern the spatial distributions of SL surface states. More specifically, the existence of well-localized levels near the bulk miniband edges has been demonstrated, which is (to the best of our knowledge) a new result with respect to single-band SL descriptions. It has also been shown that due to the mixing of Γ-valley- and *X*-valley-derived minibands, SL surface states can either be predominantly confined to the outermost GaAs layer (Γ-like surface states) or localized mostly at the outermost AlAs layer (*X*-like surface states), or possibly exhibit a hybridized Γ-*X* nature. Moreover, by just a slight variation of the clad-layer parameters, a Γ-*X* crossover of the character of SL surface states, resulting in a dramatic change of their localization properties, can be induced. These predictions might be verified, e.g., by photoemission spectroscopy, whose yield is extremely sensitive to the existence and spatial distributions of SL surface states, so the layer-resolved photocurrent allows to identify excitations from individual SL layers in the subsurface SL region.[29,30]

ACKNOWLEDGMENTS

This work has been supported by the University of Wrocław with the Grant No. 2016/W/IFD/02.

*Electronic address: rku@ifd.uni.wroc.pl

[1] G. Bastard, *Wave Mechanics Applied to Semiconductor Heterostructures* (Les Éditions de Physique, Les Ulis, 1988).
[2] P.-F. Yuh and K.L. Wang, Phys. Rev. B **38**, 13 307 (1988).
[3] H. Ohno, E.E. Mendez, J.A. Brum, J.M. Hong, F. Agulló-Rueda, L.L. Chang, and L. Esaki, Phys. Rev. Lett. **64**, 2555 (1990).
[4] H. Ohno, E.E. Mendez, A. Alexandrou, and J.M. Hong, Surf. Sci. **267**, 161 (1992).
[5] M. Stęślicka, R. Kucharczyk, A. Akjouj, B. Djafari-Rouhani, L. Dobrzynski, and S.G. Davison, Surf. Sci. Rep. **47**, 93 (2002).
[6] D.M. Wood and A. Zunger, Phys. Rev. B **53**, 7949 (1996).
[7] H.C. Liu, Appl. Phys. Lett. **51**, 1019 (1987).
[8] N.J. Pulsford, R.J. Nicholas, P. Dawson, K.J. Moore, G. Duggan, and C.T.B. Foxon, Phys. Rev. Lett. **63**, 2284 (1989).
[9] V. Voliotis, R. Grousson, P. Lavallard, E.L. Ivchenko, A.A. Kiselev, and R. Planel, Phys. Rev. B **49**, 2576 (1994).
[10] M. Nakayama, K. Imazawa, K. Suyama, I. Tanaka, and H. Nishimura, Phys. Rev. B **49**, 13 564 (1994).
[11] R. Teissier, J.J. Finley, M.S. Skolnick, J.W. Cockburn, J.-L. Pelouard, R. Grey, G. Hill, M.A. Pate, and R. Planel, Phys. Rev. B **54**, R8329 (1996).
[12] C. Gourdon, D. Martins, P. Lavallard, E.L. Ivchenko, Y.-L. Zheng, and R. Planel, Phys. Rev. B **62**, 16 856 (2000).
[13] C.S. Kim, A.M. Satanin, and V.B. Shtenberg, Zh. Éksp. Teor. Fiz. **118**, 413 (2000) [JETP **91**, 361 (2000)].
[14] I.C. da Cunha Lima, A. Ghazali, and P.D. Emmel, Phys. Rev. B **54**, 13 996 (1996).
[15] In accordance with Ref. 19, the longitudinal effective mass along the [001] direction of the (anisotropic) *X* valley, i.e., for the X_z valley, is considered in Eq. (2b).
[16] T. Ando and H. Akera, Phys. Rev. B **40**, 11 619 (1989).
[17] J.-B. Xia, Phys. Rev. B **41**, 3117 (1990).
[18] M.U. Erdoğan, K.W. Kim, M.A. Stroscio, and M. Dutta, J. Appl. Phys. **74**, 4777 (1993).
[19] Note that out of all the *X* states, only the X_z-valley ones are elastically coupled to Γ states in (001)-oriented GaAs/AlAs heterostructures with perfect interfaces (see, e.g., Ref. 11).
[20] Y. Fu, M. Willander, E.L. Ivchenko, and A.A. Kiselev, Phys. Rev. B **47**, 13 498 (1993).
[21] J.P. Cuypers and W. van Haeringen, Phys. Rev. B **48**, R11 469 (1993).
[22] B.A. Foreman, Phys. Rev. Lett. **81**, 425 (1998).
[23] The bulk dispersion relation of a GaAs/AlAs SL described by a two-band envelope-function model with δ-functional Γ-*X* coupling is explicitly given, e.g., in Ref. 17, whereas the wave functions at SL miniband edges are examined, e.g., in Ref. 18.
[24] J.N. Schulman and Y.-C. Chang, Phys. Rev. B **24**, 4445 (1981).
[25] I. Bartoš and S.G. Davison, Phys. Rev. B **32**, 7863 (1985).
[26] K.A. Mäder and A. Zunger, Phys. Rev. B **50**, 17 393 (1994).
[27] R. Kucharczyk, U. Freking, P. Krüger, and J. Pollmann, Surf. Sci. **482-485**, 612 (2001).
[28] In fact, the Γ-*X* intervalley mixing slightly enhances the dispersion of the lowest miniband, thus increasing its bandwidth. The tiny shift of the first miniband bottom (at $k=0$) toward lower energies (by about 0.7 meV) is noticeable in the inset to Fig. 2.
[29] T. Strasser, C. Solterbeck, W. Schattke, I. Bartoš, M. Cukr, P. Jiříček, C.S. Fadley, and M.A. Van Hove, Phys. Rev. B **63**, 195321 (2001).
[30] I. Bartoš, T. Strasser, and W. Schattke, Surf. Sci. **507-510**, 160 (2002).